Lecture 9: Gerrit Lohmann

ALFRED-WEGENER-INSTITUT
HELMHOLTZ-ZENTRUM FÜR POLAR-
UND MEERESFORSCHUNG

Mathematical Modeling of the Earth System

Earth system models including tracers and dynamical vegetation

Cryosphere (Sea ice, ice sheets, and permafrost)

Random Systems (Stochastic equations, Lattice Gases)

July 13, 2023

Weather

Climate

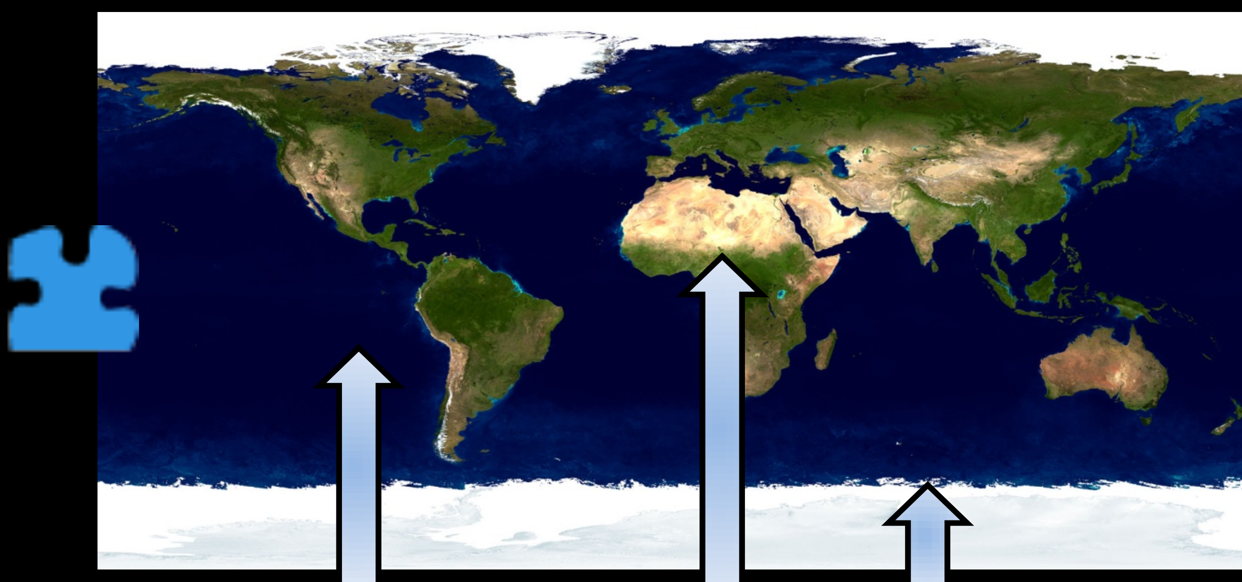

Oceans, land, Ice

Earth System

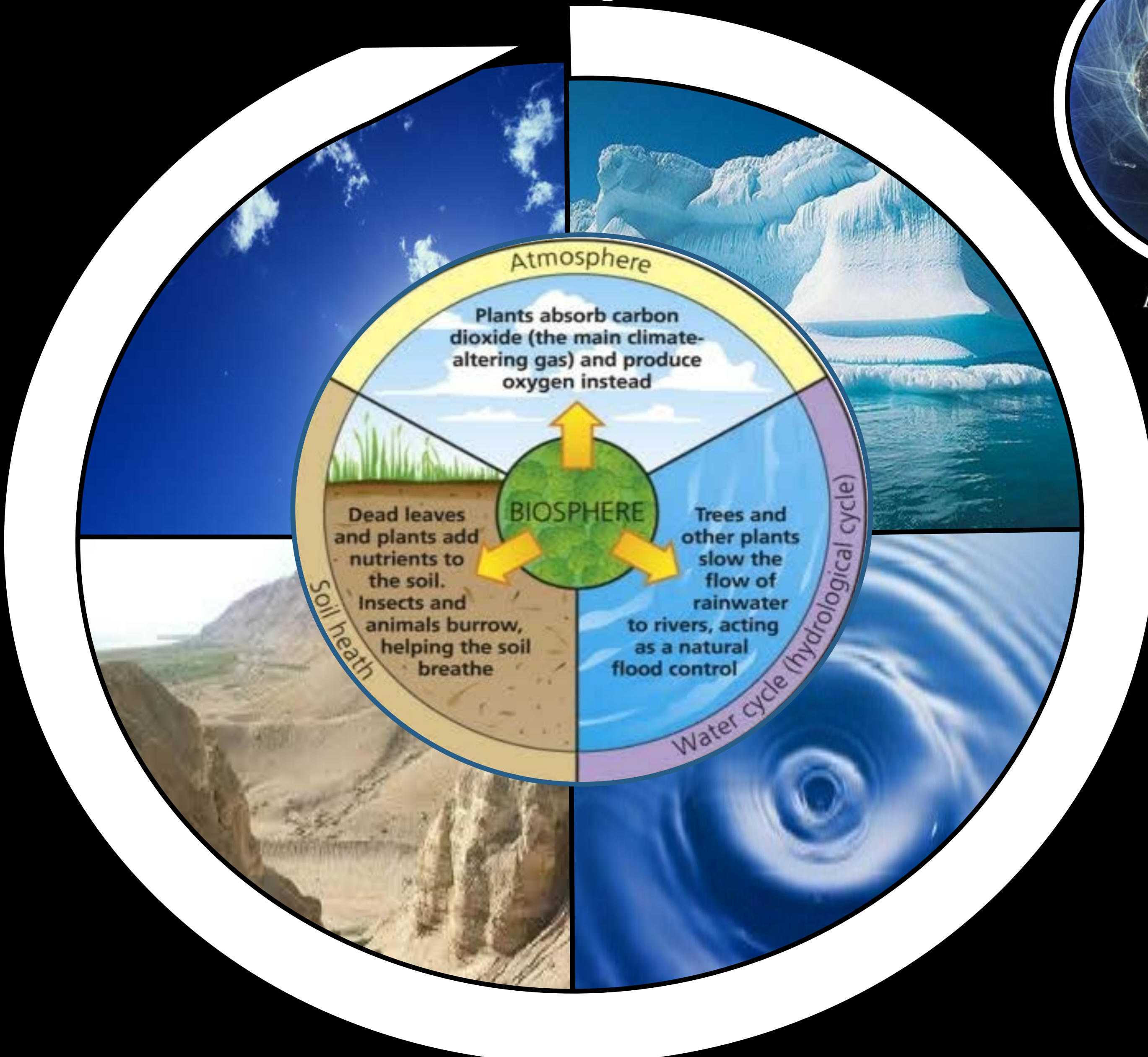

ANTHROPOSPHERE

Mathematical Modelling

Classes of models

Ordinary diffential eq. (Box models)
Partial diffential eq. (Diffusion & Advection)
Stochastic (different time & length scales)
Discrete dynamics (e.g., Population dynamics)

Examples of Resolution
(global spectral model, zoom onto Europe)

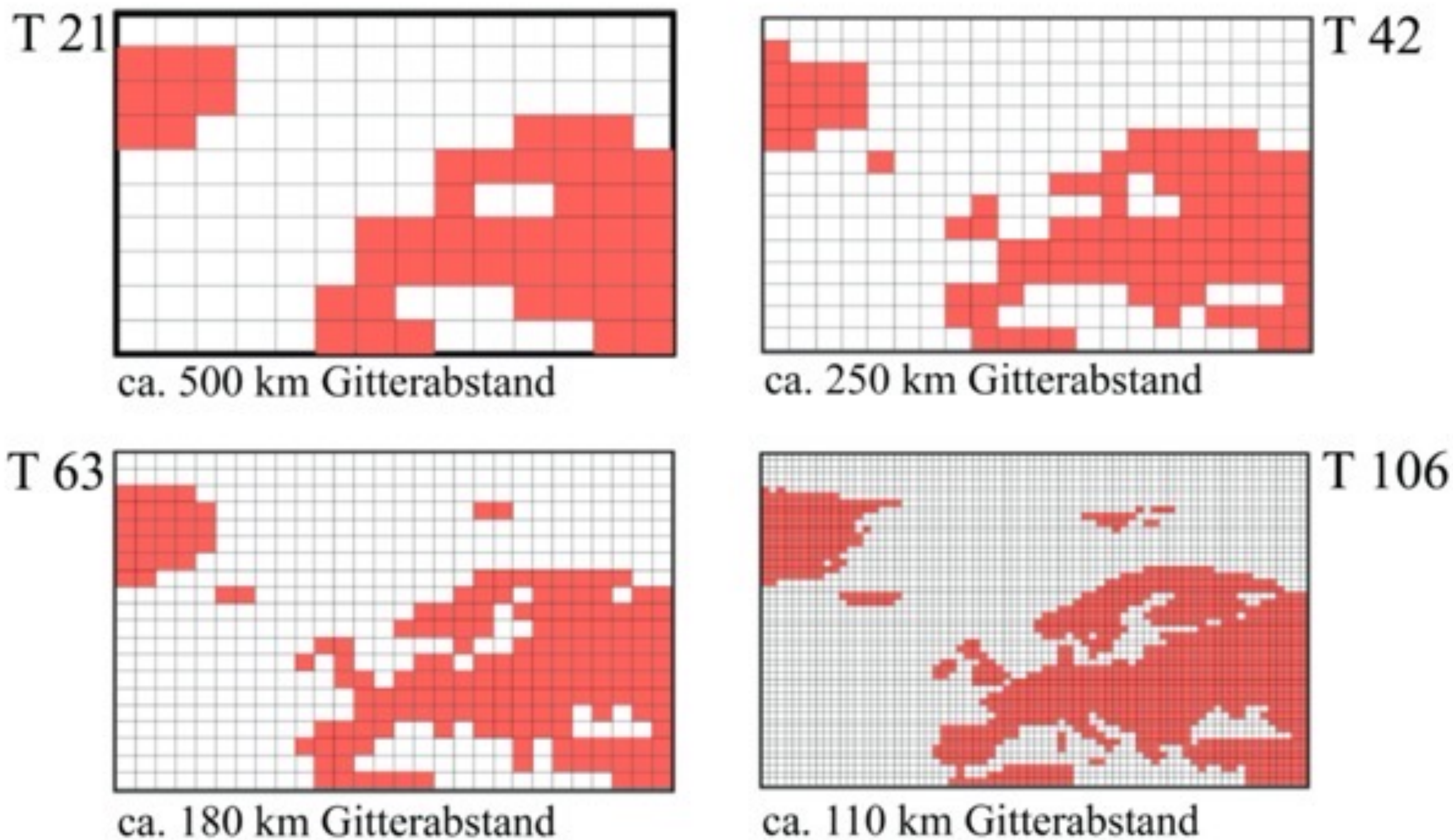

Ocean circulation models and boundary conditions

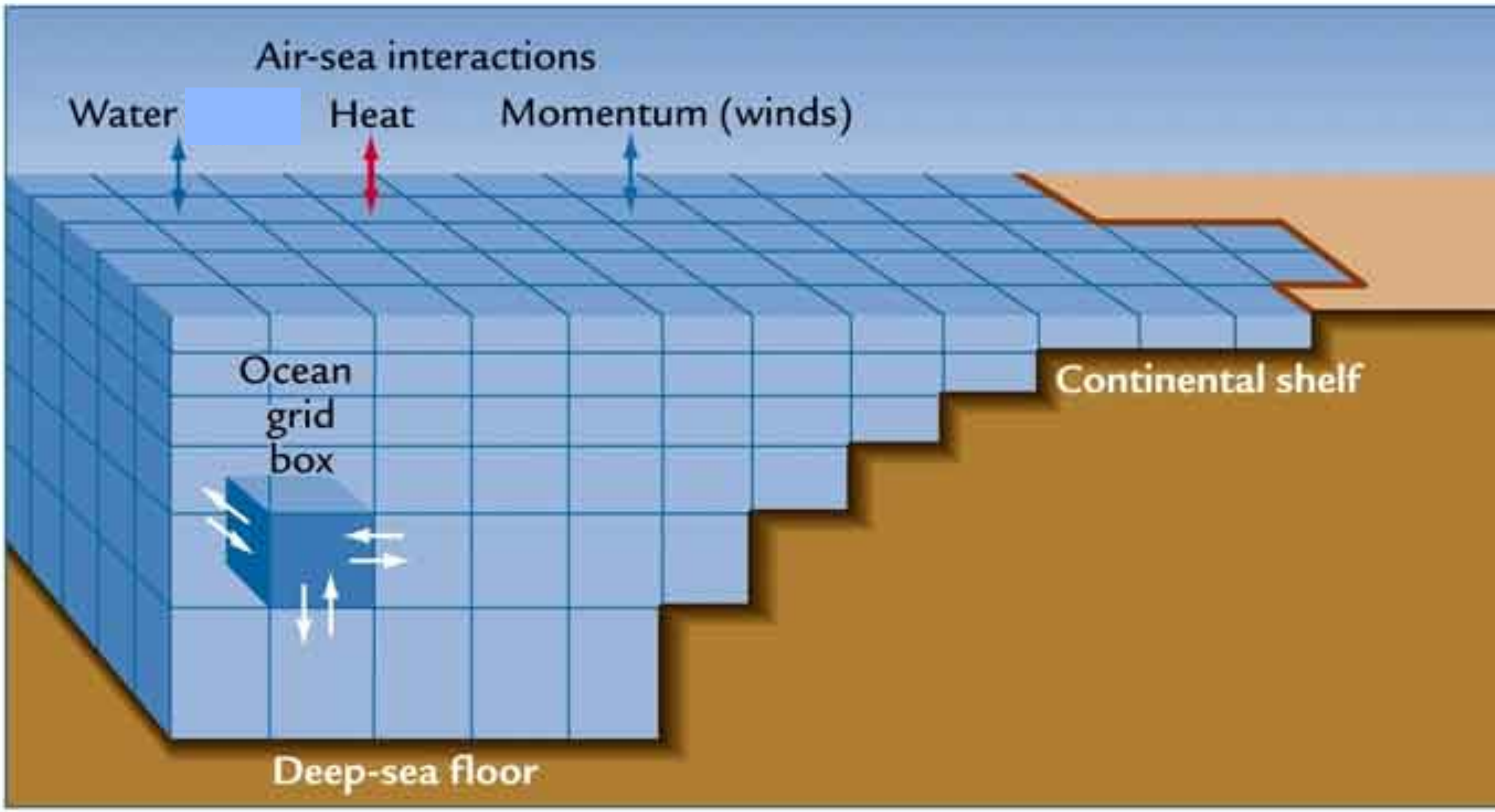

Energy balance model: Concepts of climate

$$(1-\alpha)S\pi R^2 = 4\pi R^2 \epsilon\sigma T^4$$

$$T = \sqrt[4]{\frac{(1-\alpha)S}{4\epsilon\sigma}}$$

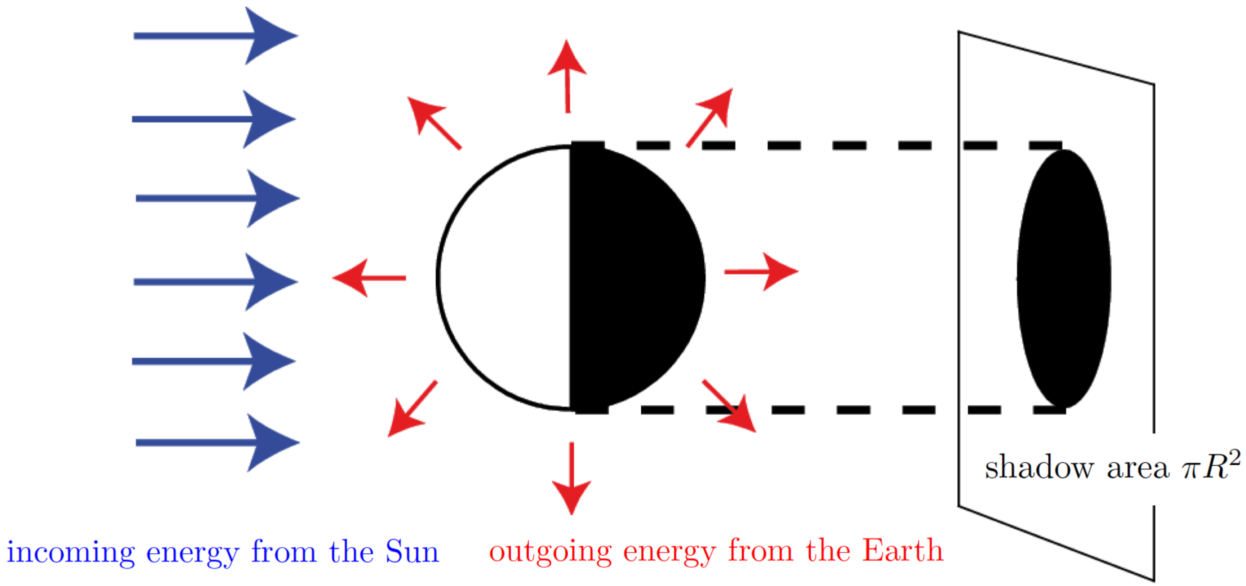

Heat capacity of the climate system

Fast rotation

Lohmann, 2020

Euler integrator

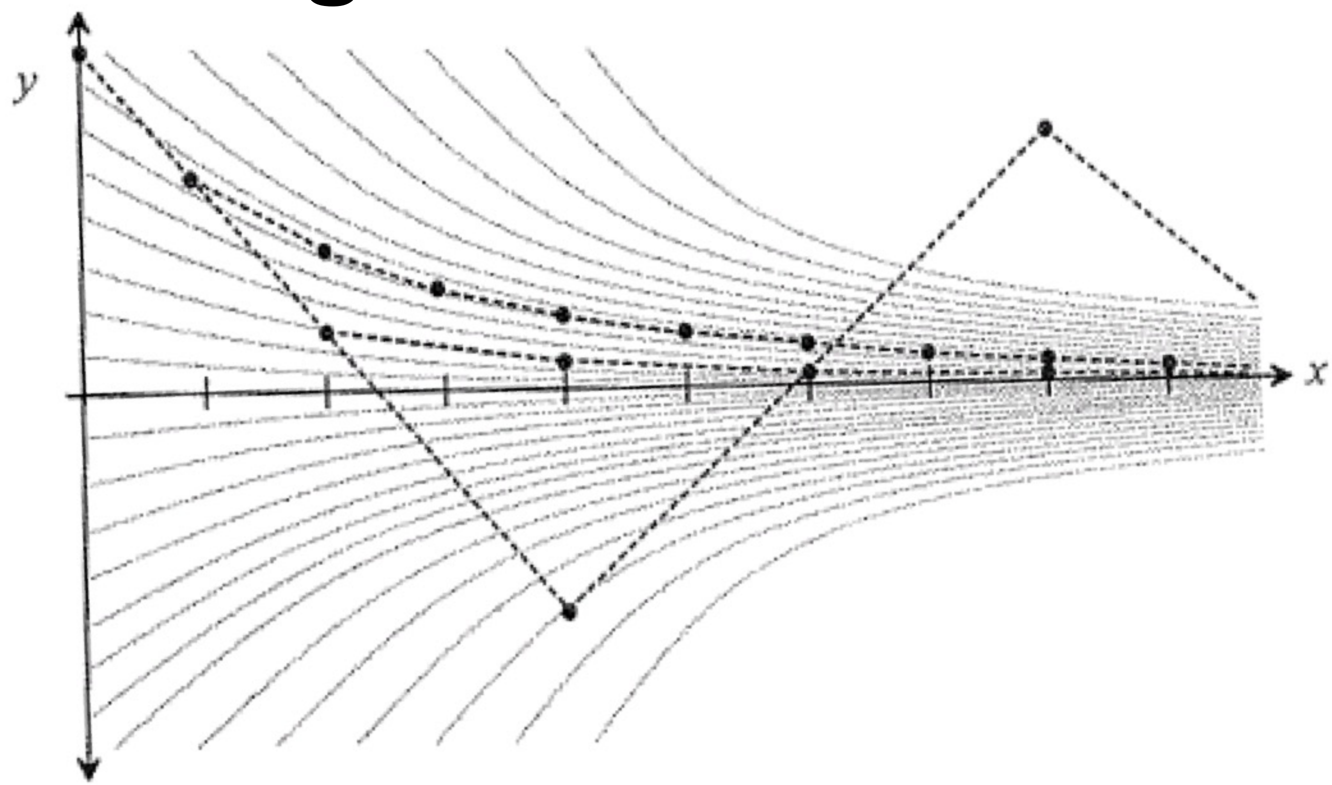

Figure 6.2. Origin of oscillation in the Euler method. The gray lines show the family of solutions of $dy/dx = Ay$, and the dotted lines show the numerical solution for various step sizes.

This algorithm approximates the point computation by this formula

$p_{k+1} = p_k + h * v(p_k)$

where *h* specifies the *integration step.*

The streamline is then constructed by successive integration.

Finite differences: Diffusion-advection

$$\frac{\partial C(x,t)}{\partial t} + u\frac{\partial C(x,t)}{\partial x} = \kappa\frac{\partial^2 C(x,t)}{\partial x^2} \qquad (1)$$

Finite differences: Diffusion-advection

$$\frac{\partial C(x,t)}{\partial t} + u\frac{\partial C(x,t)}{\partial x} = \kappa\frac{\partial^2 C(x,t)}{\partial x^2} \tag{1}$$

Approximate the derivatives using the centered difference scheme:

j-index for time

$$\frac{\partial C_{i,j}}{\partial t} \approx \frac{C_{i,j+1} - C_{i,j-1}}{2\Delta t} \tag{2}$$

i-index for space

$$\frac{\partial C_{i,j}}{\partial x} \approx \frac{C_{i+1,j} - C_{i-1,j}}{2\Delta x} \tag{3}$$

$$\frac{\partial^2 C_{i,j}}{\partial x^2} \approx \frac{C_{i+1,j} - 2C_{i,j} + C_{i-1,j}}{\Delta x^2} \tag{4}$$

Finite differences Diffusion-advection

$$\frac{\partial C(x,t)}{\partial t} + u\frac{\partial C(x,t)}{\partial x} = \kappa\frac{\partial^2 C(x,t)}{\partial x^2} \qquad (1)$$

Approximate the derivatives using the centered difference scheme:

j-index for time

$$\frac{\partial C_{i,j}}{\partial t} \approx \frac{C_{i,j+1} - C_{i,j-1}}{2\Delta t} \qquad (2)$$

$$\frac{\partial C_{i,j}}{\partial x} \approx \frac{C_{i+1,j} - C_{i-1,j}}{2\Delta x} \qquad (3)$$

i-index for time

$$\frac{\partial^2 C_{i,j}}{\partial x^2} \approx \frac{C_{i+1,j} - 2C_{i,j} + C_{i-1,j}}{\Delta x^2} \qquad (4)$$

Inserting (2)-(4) into (1) gives

$$\frac{C_{i,j+1} - C_{i,j-1}}{2\Delta t} + u\frac{C_{i+1,j} - C_{i-1,j}}{2\Delta x} \approx \kappa\frac{C_{i+1,j-1} - 2C_{i,j-1} + C_{i-1,j-1}}{\Delta x^2} \qquad (5)$$

(Note that we evaluate the diffusion term at time $j-1$ instead of time j to avoid numerical instability.) Rephrasing

Finite differences: Diffusion-advection

$$\frac{\partial C(x,t)}{\partial t} + u\frac{\partial C(x,t)}{\partial x} = \kappa\frac{\partial^2 C(x,t)}{\partial x^2} \quad (1)$$

Approximate the derivatives using the centered difference scheme:

$$\frac{\partial C_{i,j}}{\partial t} \approx \frac{C_{i,j+1} - C_{i,j-1}}{2\Delta t} \quad (2)$$

$$\frac{\partial C_{i,j}}{\partial x} \approx \frac{C_{i+1,j} - C_{i-1,j}}{2\Delta x} \quad (3)$$

$$\frac{\partial^2 C_{i,j}}{\partial x^2} \approx \frac{C_{i+1,j} - 2C_{i,j} + C_{i-1,j}}{\Delta x^2} \quad (4)$$

Inserting (2)-(4) into (1) gives

$$\frac{C_{i,j+1} - C_{i,j-1}}{2\Delta t} + u\frac{C_{i+1,j} - C_{i-1,j}}{2\Delta x} \approx \kappa\frac{C_{i+1,j-1} - 2C_{i,j-1} + C_{i-1,j-1}}{\Delta x^2} \quad (5)$$

(Note that we evaluate the diffusion term at time $j-1$ instead of time j to avoid numerical instability.) Rephrasing

Leapfrog scheme

$$C_{i,j+1} \approx C_{i,j-1} - u\frac{\Delta t}{\Delta x}(C_{i+1,j} - C_{i-1,j}) + \kappa\frac{2\Delta t}{\Delta x^2}(C_{i+1,j-1} - 2C_{i,j-1} + C_{i-1,j-1}) \quad (6)$$

Finite differences: Diffusion-advection

$$\frac{\partial C(x,t)}{\partial t} + u\frac{\partial C(x,t)}{\partial x} = \kappa \frac{\partial^2 C(x,t)}{\partial x^2}$$

Leap-Frog Scheme (CTCS Scheme)

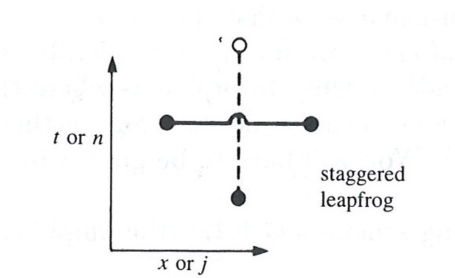

The leap-frog scheme is second order in time and space,

$$T_i^{n+1} = T_i^{n-1} - \frac{V\Delta t}{\Delta x}\left(T_{i+1}^n - T_{i-1}^n\right)$$

but it requires that the two last time levels are kept in memory.

Leapfrog scheme

$$C_{i,j+1} \approx C_{i,j-1} - u\frac{\Delta t}{\Delta x}(C_{i+1,j} - C_{i-1,j}) + \kappa\frac{2\Delta t}{\Delta x^2}(C_{i+1,j-1} - 2C_{i,j-1} + C_{i-1,j-1})$$

Finite differences: Diffusion-advection

$$\frac{\partial C(x,t)}{\partial t} + u\frac{\partial C(x,t)}{\partial x} = \kappa\frac{\partial^2 C(x,t)}{\partial x^2} \quad (1)$$

Leap-Frog Scheme (CTCS Scheme)

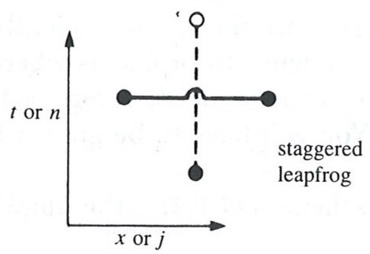

The leap-frog scheme is second order in time and space,

$$T_i^{n+1} = T_i^{n-1} - \frac{V\Delta t}{\Delta x}\left(T_{i+1}^n - T_{i-1}^n\right)$$

but it requires that the two last time levels are kept in memory.

Chess Board for Leap-Frog

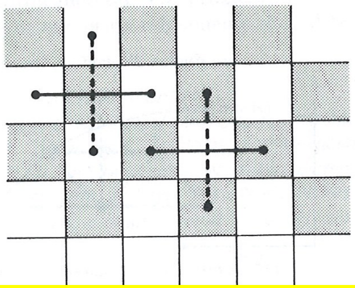

Leap-frog is stable, provided CFL-criterium is fulfilled, less diffusive than upwind, but leads to oscillations, especially at sharp gradients. There can be a decoupling of two solutions!

Leapfrog scheme

$$C_{i,j+1} \approx C_{i,j-1} - u\frac{\Delta t}{\Delta x}(C_{i+1,j} - C_{i-1,j}) + \kappa\frac{2\Delta t}{\Delta x^2}(C_{i+1,j-1} - 2C_{i,j-1} + C_{i-1,j-1}) \quad (6)$$

Shallow Water Model

Rossby and gravity waves

$$
\begin{aligned}
\partial_t u &= f\,v - g\,\partial_x \eta \\
\partial_t v &= -f\,u - g\,\partial_y \eta \\
\partial_t \eta &= -\partial_x (H u) - \partial_y (H v)
\end{aligned}
$$

```
u.new[ia.0,ia.0]<-u.old[ia.0,ia.0]-g*dt/dx*(h[ia.p1,ia.0]-h[ia.m1,ia.0])+dt*f*v
v.new[ia.0,ia.0]<-v.old[ia.0,ia.0]-g*dt/dy*(h[ia.0,ia.p1]-h[ia.0,ia.m1])-dt*f*u
h.new[ia.0,ia.0]<-h.old[ia.0,ia.0]-H*dt*((u[ia.p1,ia.0]-u[ia.m1,ia.0])/dx + (v[ia.0,ia.p1]-
v[ia.0,ia.m1])/dy)
```

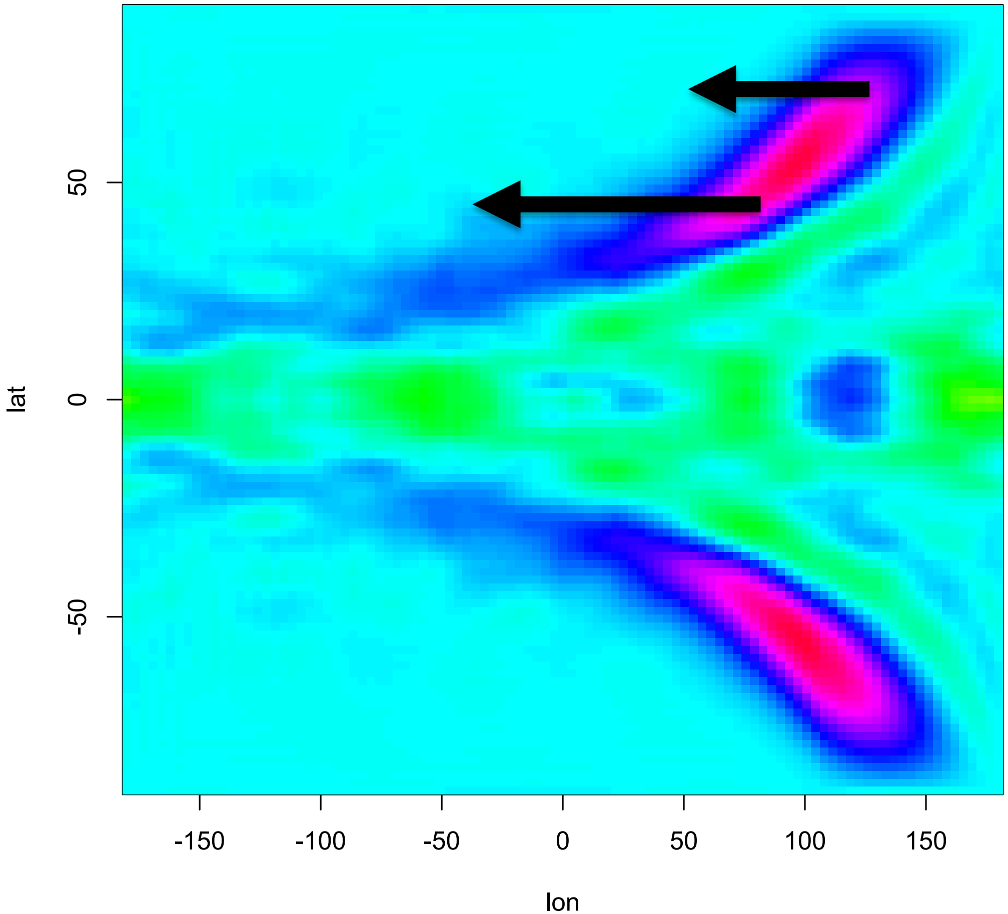

$$\omega(k,l) = -\frac{\beta k}{k^2 + l^2},$$

Figure 7.3: Global Rossby and Kelvin wave signatures in the exercise 49.

2D Staggered grids: Arakawa

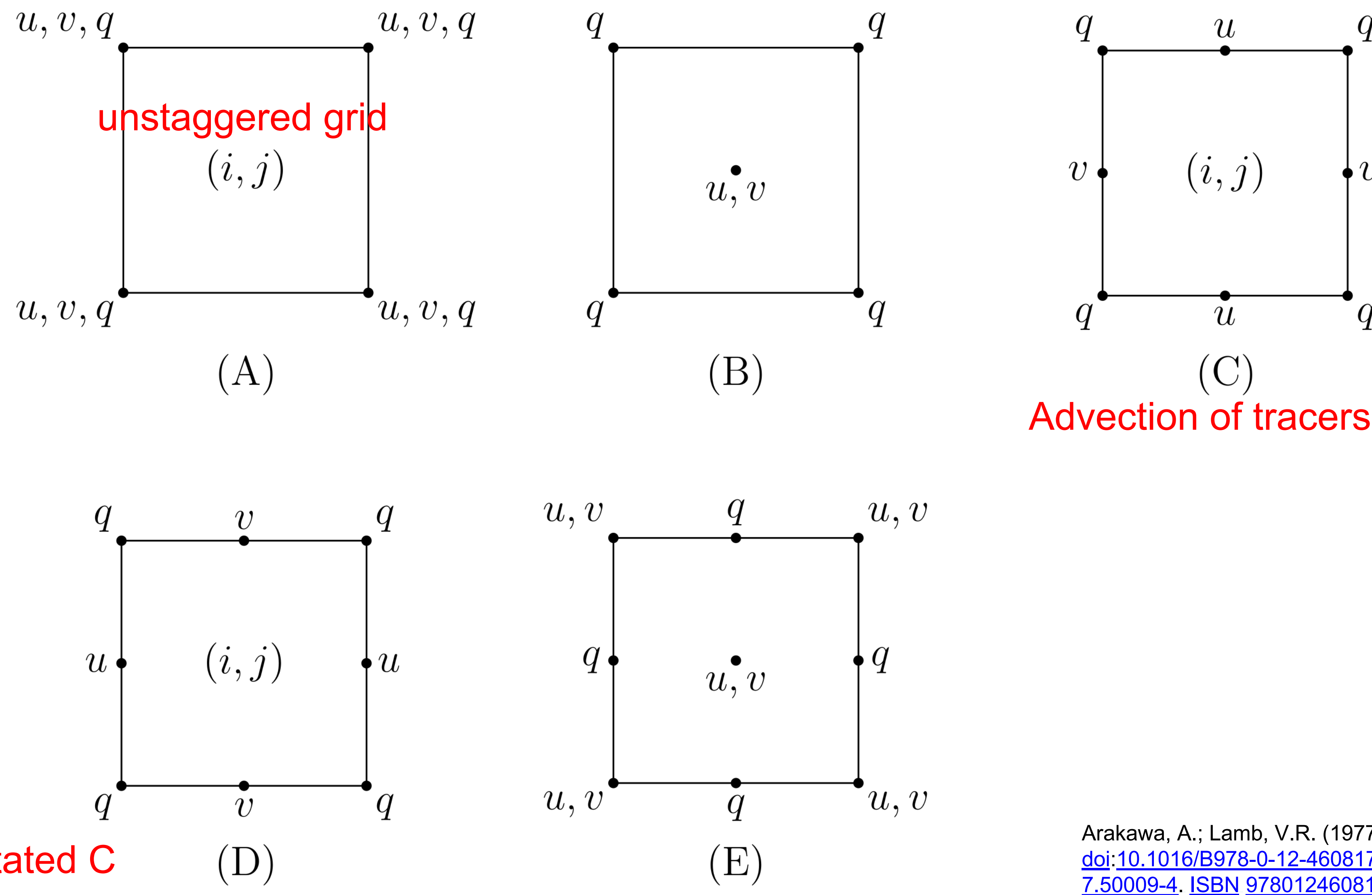

Rotated C

Arakawa, A.; Lamb, V.R. (1977) doi:10.1016/B978-0-12-460817-7.50009-4. ISBN 9780124608177.

Spectral methods

Rayleigh Bernard System
in lecture Dynamics II

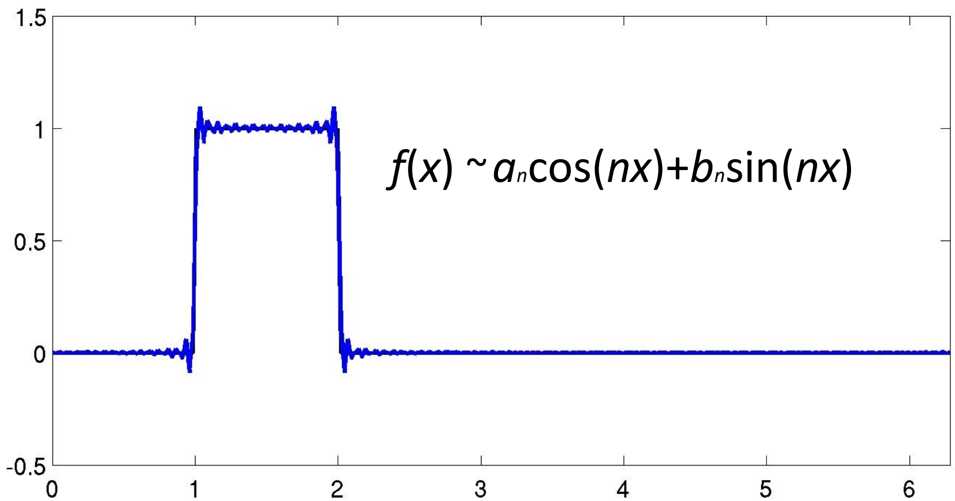

solve the diffusion equation
$\partial_t T = D\, \partial^2_x T$

Fourier–Galerkin method

used for the basis functions

the famous chaotic Lorenz model was found as a Fourier-Galerkin approximation to atmospheric convection (Lorenz, 1963)

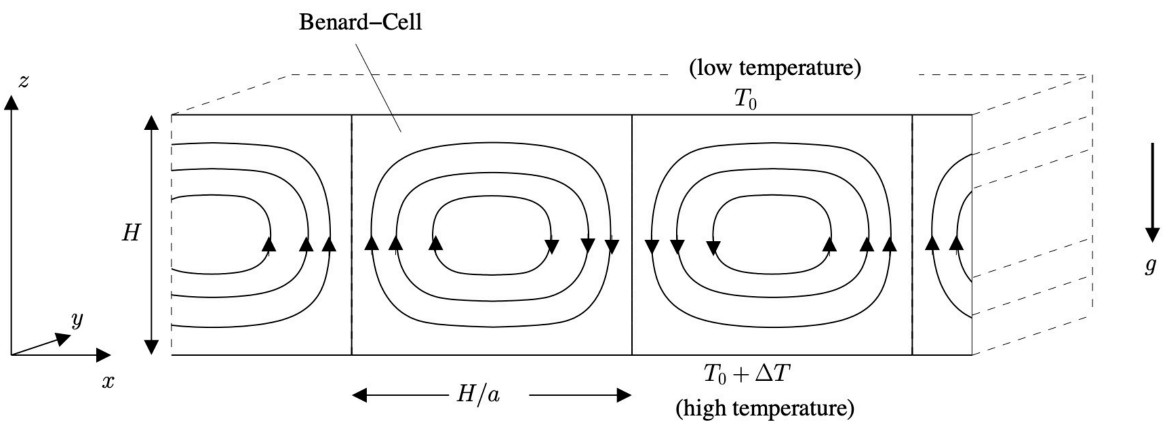

$$\Psi(x,z,t)=\sum_k\sum_l \Psi_{k,l}(t)\sin\left(k\pi a H x\right)\times\sin\left(l\pi H z\right)$$

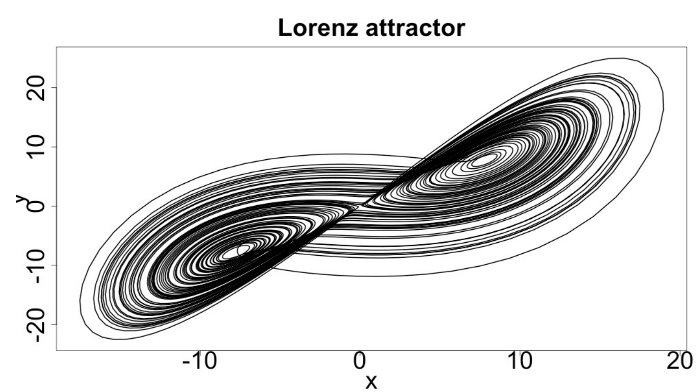

Finite differences and finite element methods

finite differences: approximate partial differential equations.
Questions to analyze and improve the stability and accuracy

Finite-difference Approximation of Derivatives

There are many ways to replace differential quotients with difference quotients, e.g.:

$$\frac{\partial T}{\partial x} \rightarrow \frac{T_j - T_{j-1}}{\Delta x} \quad \text{(backward)}$$
$$\rightarrow \frac{T_{j+1} - T_j}{\Delta x} \quad \text{(forward)}$$
$$\rightarrow \frac{T_{j+1} - T_{j-1}}{2\Delta x} \quad \text{(centered)}$$

All these tend to $\frac{\partial T}{\partial x}$ for $\Delta x \rightarrow 0$

A 2nd-order accurate Difference Quotient

in the centered difference approximation, however, we obtain from Taylor's theorem

$$\frac{T(x+\Delta x) - T(x-\Delta x)}{2\Delta x} = \frac{\partial T}{\partial x} + \frac{1}{3!}\frac{\partial^3 T}{\partial x^3}(\Delta x)^2 + \ldots$$

because the terms proportional to the second derivative cancel out. The error in the centered finite-difference approximation is of the order $(\Delta x)^2$.

Finite differences and finite element methods

As powerful as these ideas are, there are two important cases where they do not directly apply: problems that are

- described in terms of a **spatially inhomogeneous grid,**
- posed in **terms of a variational principle**.

For example, in studying the deformations, it can be most natural to describe it in **finding the minimum energy configuration**

for computational efficiency it is certainly important to match the location of the solution nodes to the shape of the body.

Ocean Model Setup in finite elements

- mesh with high resolution at deep water mass formation areas
- min. resolution ~ 6.5 km
- 41 depth level, ~ 6.000.000 3D tetrahedral elements, ~ 1.000.000 3D nodes

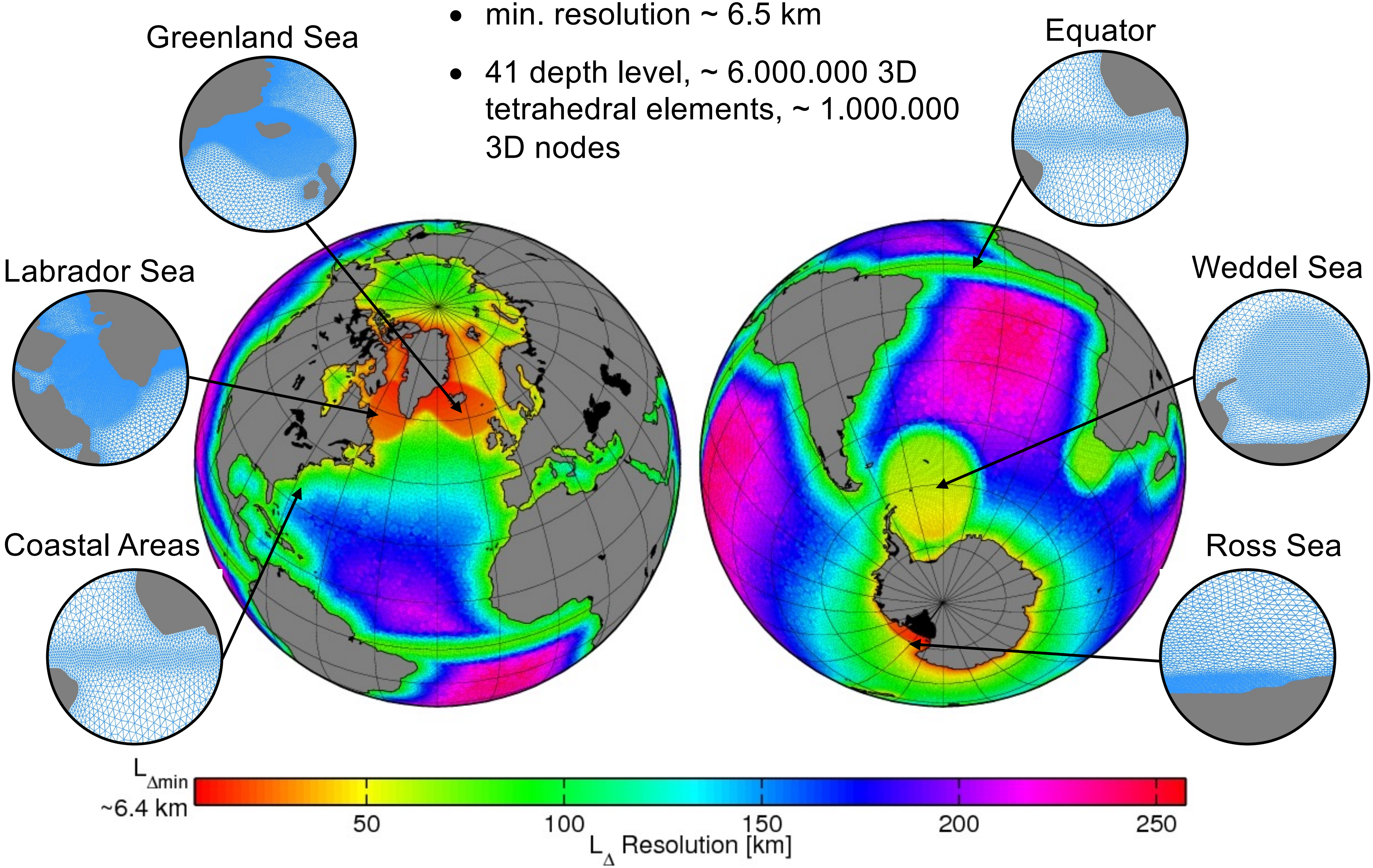

Earth System Analysis: Models

$$\frac{\partial \mathbf{v}}{\partial t} + \mathbf{v} \cdot \nabla \mathbf{v} = -2\Omega \times \mathbf{v} - \frac{1}{\rho}\nabla p + \mathbf{g} + \mathbf{F}$$

$$\frac{\partial \rho}{\partial t} + \nabla \cdot \rho \mathbf{v} = 0$$

$$\frac{\partial T}{\partial t} + \mathbf{v} \cdot \nabla T - \frac{p}{\rho^2}\frac{d\rho}{dt} = Q$$

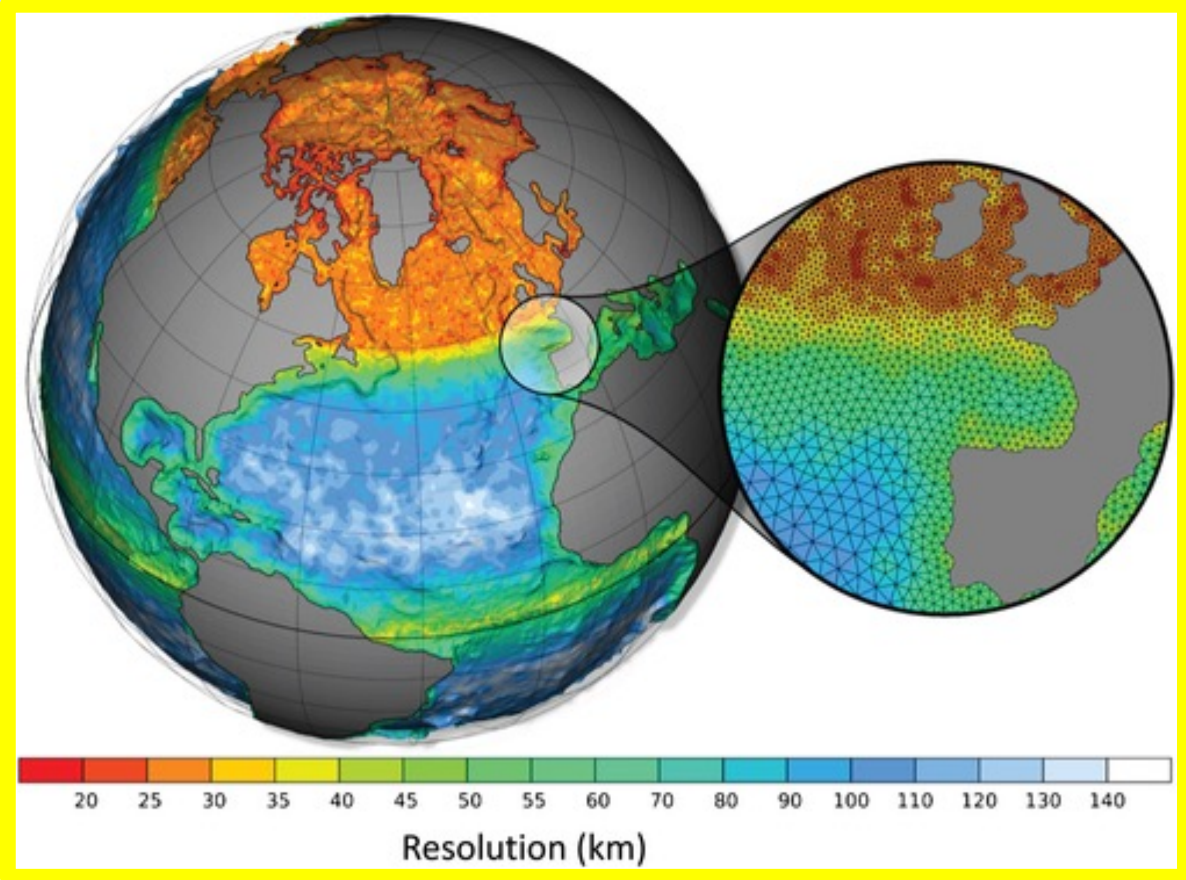

Let's return to the simple first-order flux PDE

$$\frac{\partial u}{\partial t} = -v\frac{\partial u}{\partial x} \tag{9.11}$$

to see how the Galerkin method is applied. For each basis function φ_j there is a weighted residual equation integrated over the problem domain

$$\int \left(\frac{\partial u}{\partial t} + v\frac{\partial u}{\partial x}\right) \varphi_j \, dx = 0 \tag{9.12}$$

(in this case the source term $f = 0$). Plugging in

$$u(x,t) = \sum_i a_i(t)\varphi_i(x) \tag{9.13}$$

gives

$$\sum_i \int \left(\frac{da_i}{dt}\varphi_i\varphi_j + va_i\varphi_j\frac{d\varphi_i}{dx}\right) \, dx = 0 \quad . \tag{9.14}$$

This can be written in matrix form as

$$\mathbf{A}\cdot\frac{d\vec{a}}{dt} + \mathbf{B}\cdot\vec{a} = \vec{0} \tag{9.15}$$

where

$$\mathbf{A}_{ij} = \int \varphi_i\varphi_j \, dx \tag{9.16}$$

and

$$\mathbf{B}_{ij} = v\int \varphi_j\frac{d\varphi_i}{dx} \, dx \tag{9.17}$$

are matrices that depend only on the basis functions, and the vector $\vec{a}$ is the set of expansion coefficients. This is now a system of ordinary differential equations that can be solved with the methods that we studied in Chapter 7. Since each basis function overlaps only with its immediate neighbors, the **A** and **B** matrices are very sparse and so they can be solved efficiently (this is the main job of a finite element package, and much of numerical linear algebra).

Mathematical Modelling

Classes of models

Ordinary diffential eq. (Box models)
Partial diffential eq. (Diffusion & Advection)
Stochastic (different time & length scales)
Discrete dynamics (e.g., Population dynamics)

Brownian Motion: visible under the Mikroscope: Motion of particles

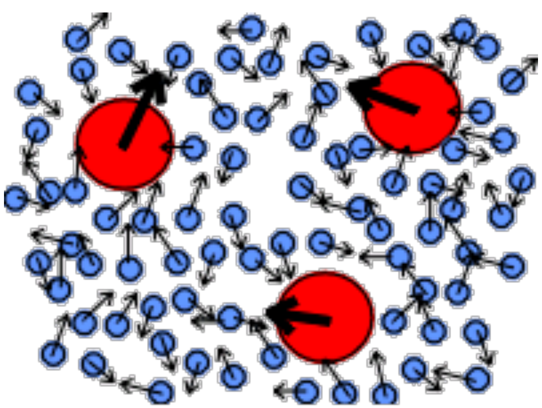

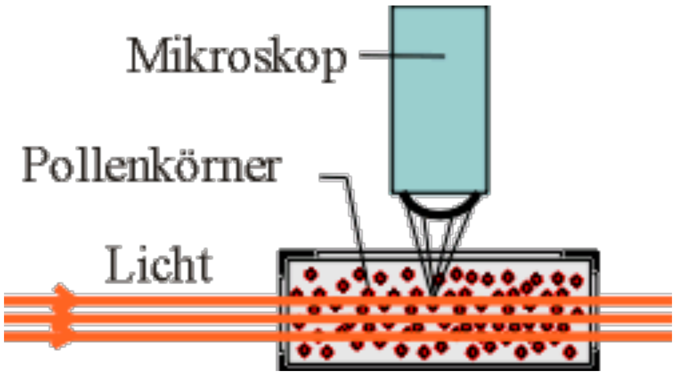

pulses, irregular
Living?
Pulses from all directions, random

Physics of the 20th century

- The matter the world is made of
- views: Elementary particles, quantum mechanics, relativity theory
- Limit of divisibility (Democritus, Aristotle): Matter is not a continuous whole: "The world cannot be composed of infinitely small particles".

HELMHOLTZ

Brownian Motion

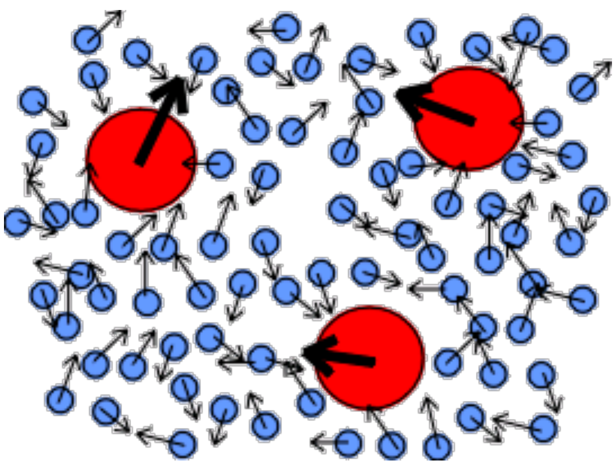

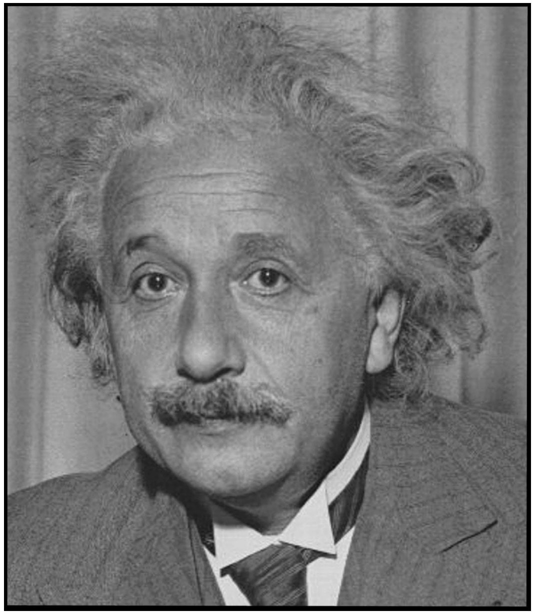

Einstein,Orstein, Uhlenbeck, Wiener, Fokker, Planck et al.

dx/dt = f(x) + g(x) dw/dt

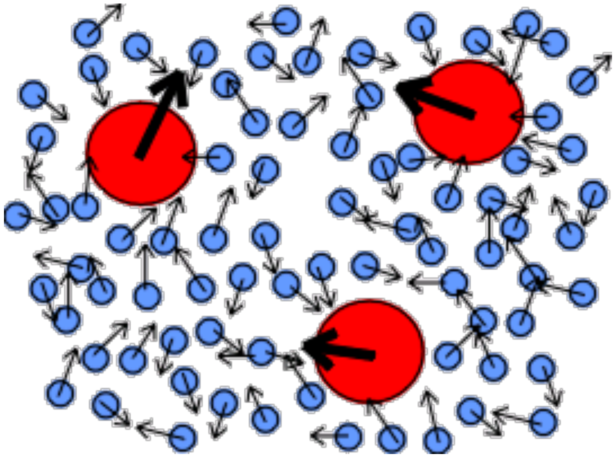

Brownian motion

is the random movement of particles, caused by their bombardment on all sides by bigger molecules.

This motion can be seen in the behavior of pollen grains placed in a glass of water

Because this motion often drives the interaction of time and spatial scales, it is important in several fields.

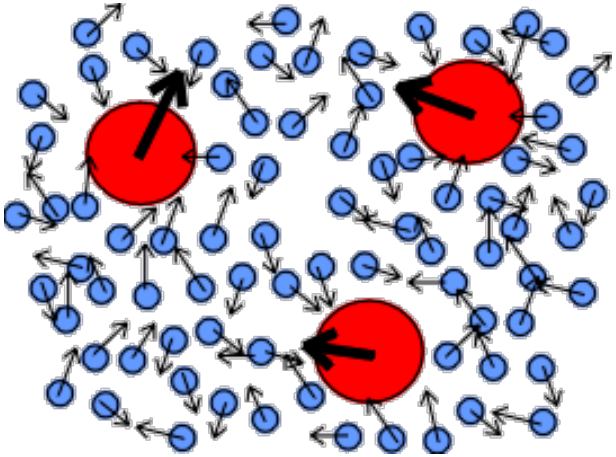

Following an idea of Hasselmann one can divide the climate dynamics into two parts. These two parts are the slowly changing climate part and rapidly changing weather part. **The** weather part can be modeled by a stochastic process such as white noise

Climate variability

- Brownian Particle: Climate
- Molecules: Weather

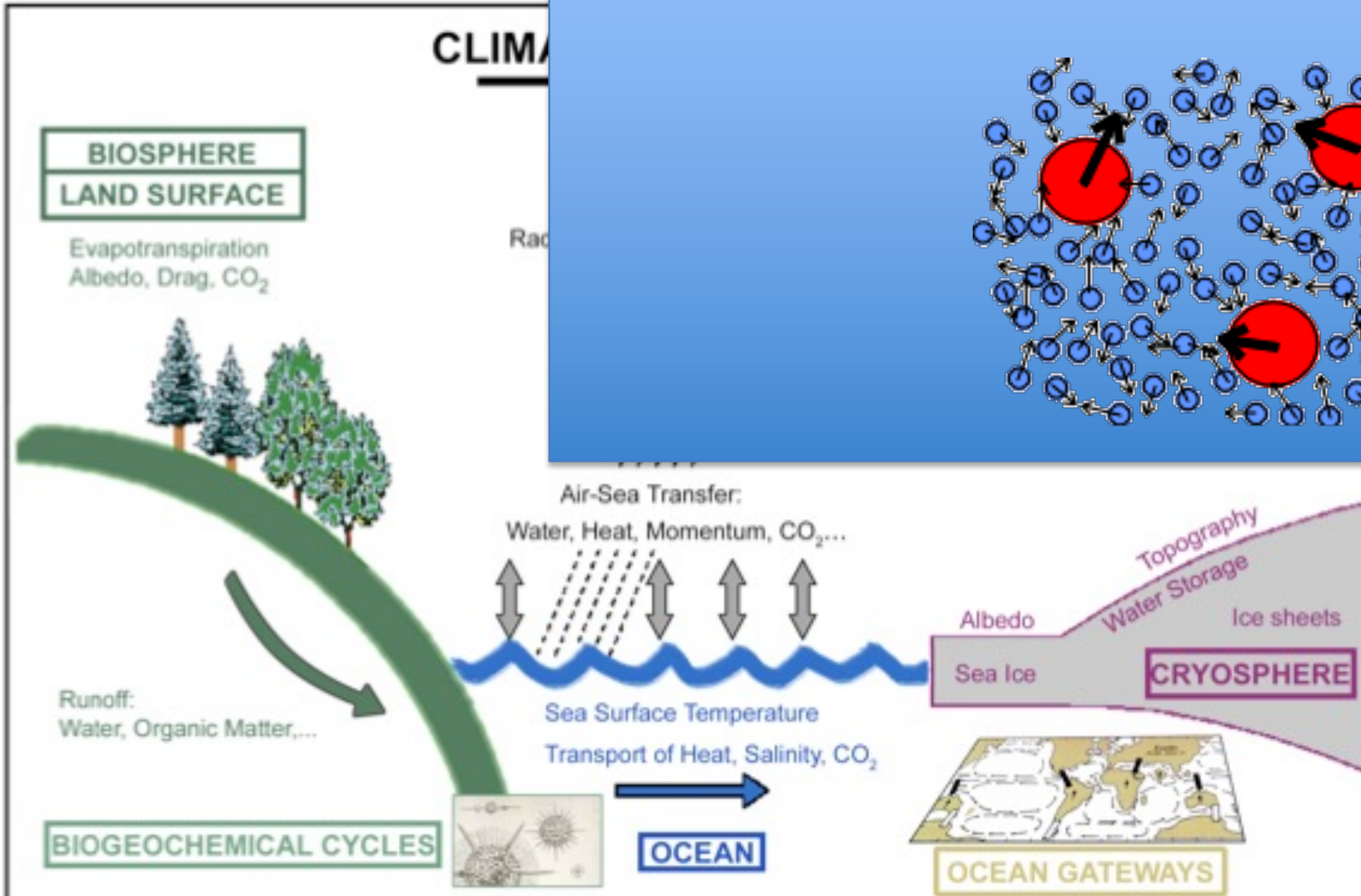

Das Klimaproblem aus physikalischer Sicht

Climate

Brownsche Partikel: Klim

Moleküle: Wetter

Probabilities

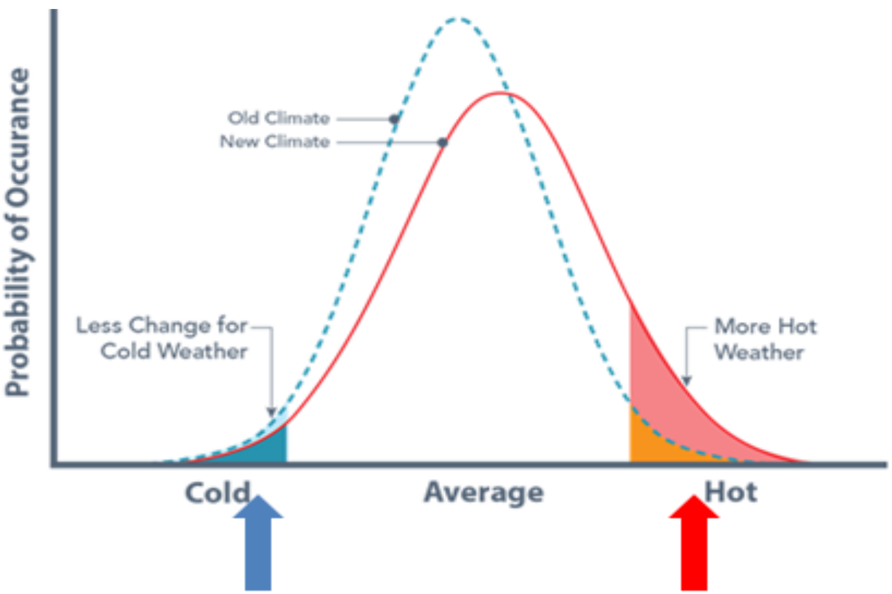

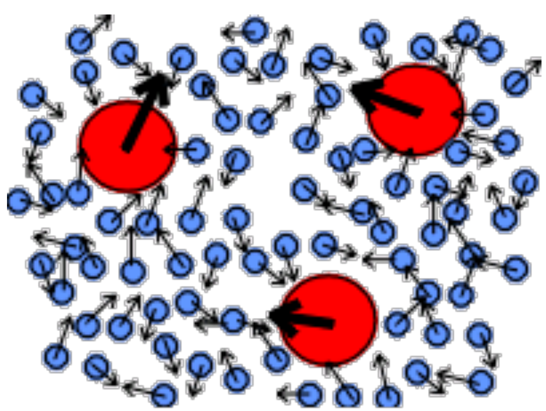

Predictability

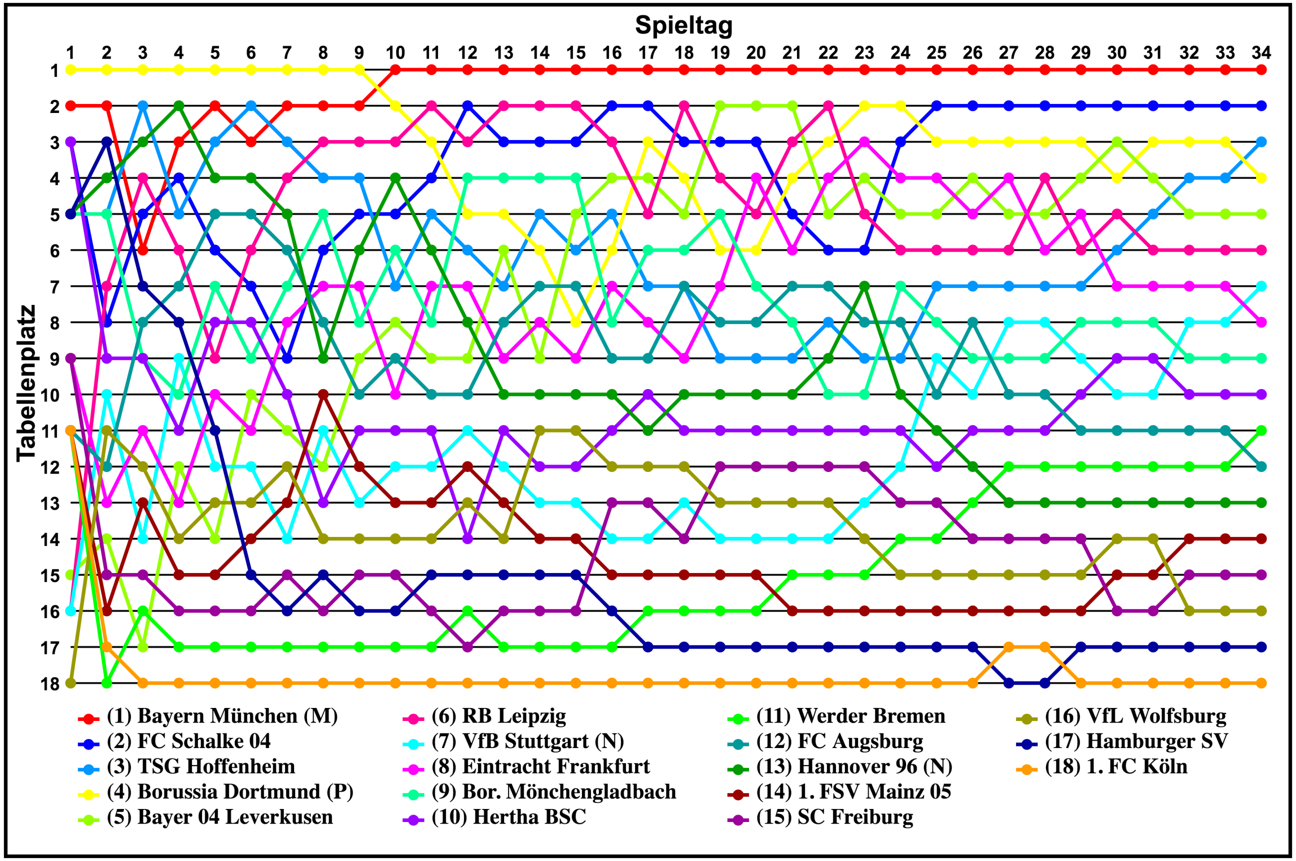

Coarse graining -> Stochastic

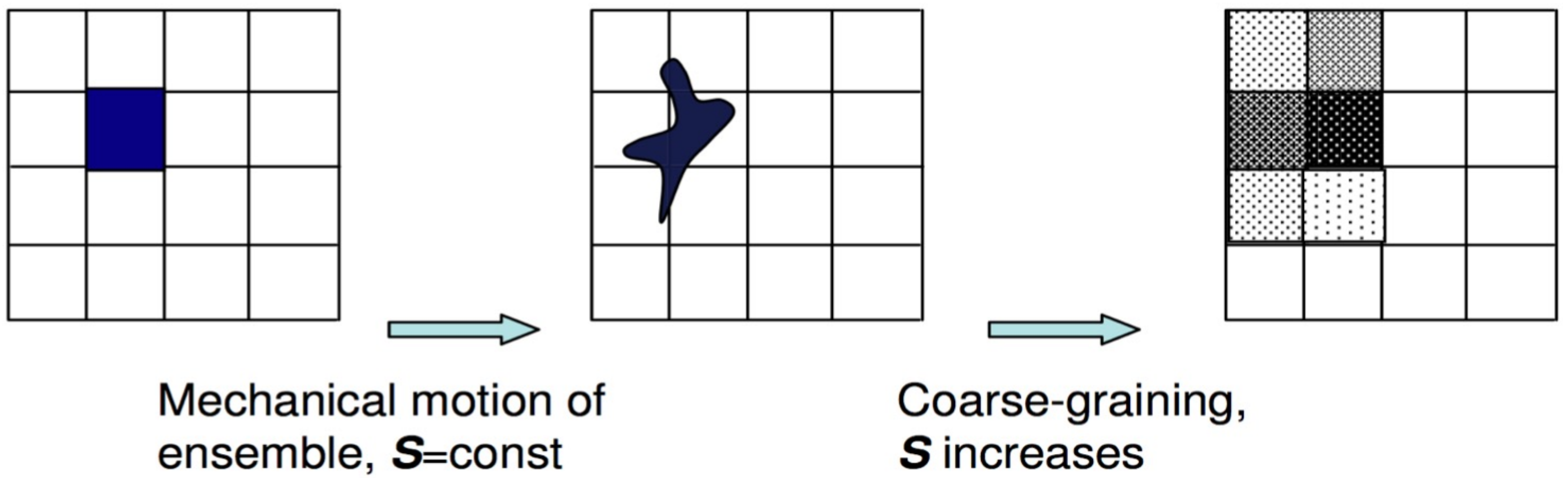

Figure 8.11: The Ehrenfests coarse-graining: two motion - coarse-graining cycles in 2D (values of probability density are presented by hatching density).

Lattice Boltzmann Method

- Simple “mesoscopic” rules yield complex behavior
- Recently established as CFD alternative in engineering
- Have been proven to simulate Navier-Stokes equations
- Velocity space discretized
- Explicit method, simple update rule:

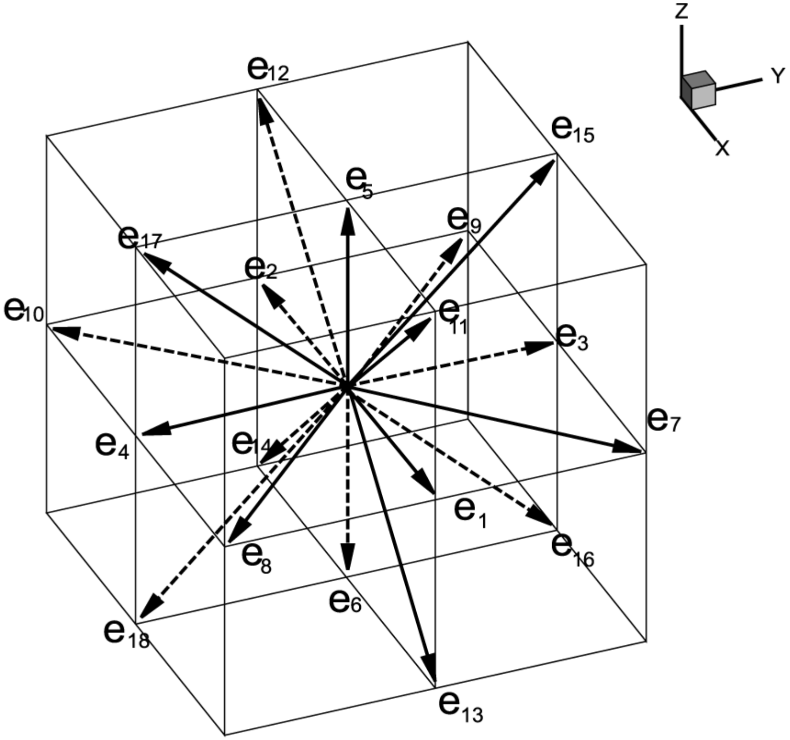

$$f_i(\vec{x} + \vec{e}_i, t+1) = f_i(\vec{x}, t) - \frac{f_i - f_i^{eq}}{\tau} + F_i$$

$$f_i^{eq} = \rho w_i \left[1 + 3(\vec{e}_i \cdot \vec{v}) + \frac{9}{2}(\vec{e}_i \cdot \vec{v})^2 - \frac{3}{2}\vec{v}^2 \right]$$

Force terms

Function of Fluid viscosity

LBM (cont'd)

- Low per-gridpoint update cost
- Easy parallelization
- 2nd-order accuracy (space checked for 3D Poiseuille flow
- Smagorinsky turbulence model included
- Developing refinements o LBM for oceanography

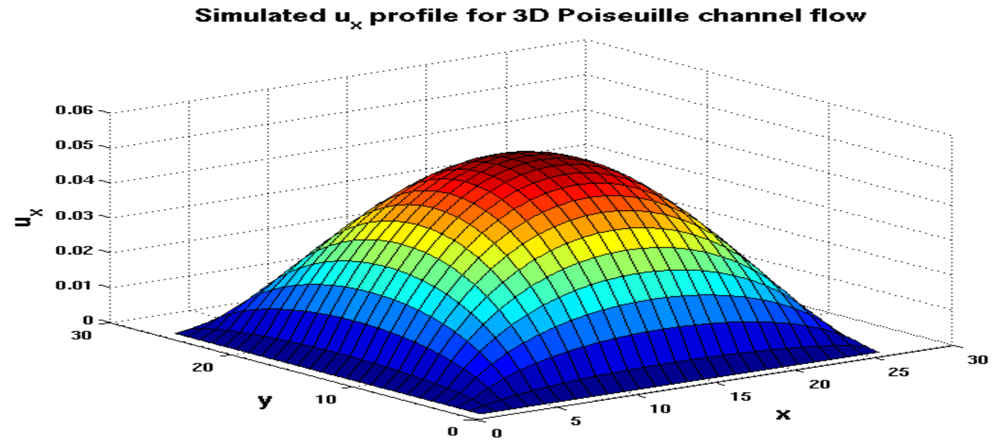

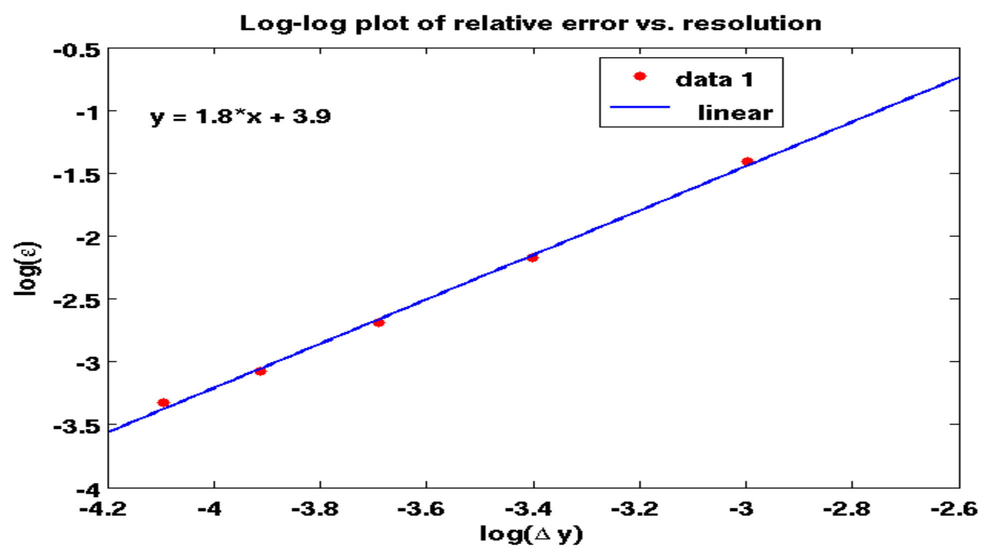

The simplest random system consists of values x taken from a distribution $p(x)$. For example, in a coin toss x can be heads or tails, and $p(\text{heads}) = p(\text{tails}) = 1/2$. In this case x takes on discrete values; it is also possible for a random variable to come from a continuous distribution. For a continuous variable, $p(x)\,dx$ is the probability to observe a value between x and $x + dx$, and more generally

$$\int_a^b p(x)\,dx \tag{5.1}$$

is the probability to observe x between a and b.

5.1.1 Joint Distributions

Now let's consider two random variables x and y, such as the result from throwing a pair of dice, that are specified by a joint density $p(x, y)$. The expected value of a function that depends on both x and y is

$$\langle f(x,y)\rangle = \int_{-\infty}^{\infty}\int_{-\infty}^{\infty} f(x,y)\, p(x,y)\, dx\, dy \quad . \tag{5.7}$$

$p(x, y)$ must be normalized, so that

$$\int_{-\infty}^{\infty}\int_{-\infty}^{\infty} p(x,y)\, dx\, dy = 1 \quad . \tag{5.8}$$

It must also be normalized with respect to each variable, so that

$$p(x) = \int_{-\infty}^{\infty} p(x,y)\, dy \tag{5.9}$$

and

$$p(y) = \int_{-\infty}^{\infty} p(x,y)\, dx \quad . \tag{5.10}$$

Integrating a variable out of a joint distribution is called *marginalizing* over the variable.

For joint random variables a very important quantity is $p(x|y)$ ("the probability of x given y"). This is the probability of seeing a particular value of x if we already know the value of y, and is defined by *Bayes' rule*

$$p(x|y) = \frac{p(x,y)}{p(y)} \quad , \tag{5.11}$$

which takes the joint probability and divides out from it the known scalar probability. This is easily extended to combinations of more variables,

$$\begin{aligned} p(x,y,z) &= p(x|y,z)\,p(y,z) \\ &= p(x|y,z)\,p(y|z)\,p(z) \\ &= p(x,y|z)\;\;p(z) \quad , \end{aligned} \tag{5.12}$$

for independent variables $p(x|y) = p(x)p(y)/p(y) = p(x)$

"for groundbreaking contributions to our understanding of complex systems"

Ill. Niklas Elmehed © Nobel Prize Outreach

Syukuro Manabe

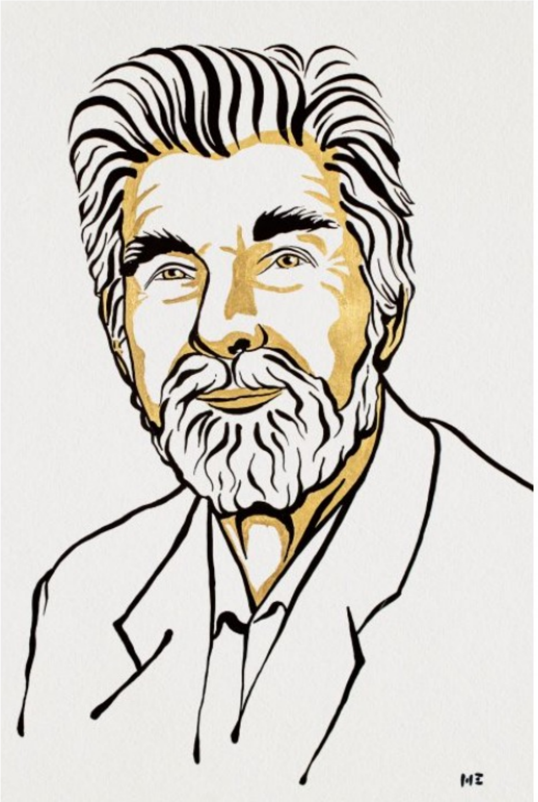

Ill. Niklas Elmehed © Nobel Prize Outreach

Klaus Hasselmann

"for the physical modelling of Earth's climate, quantifying variability and reliably predicting global warming"

Spatio-Temporal Scales

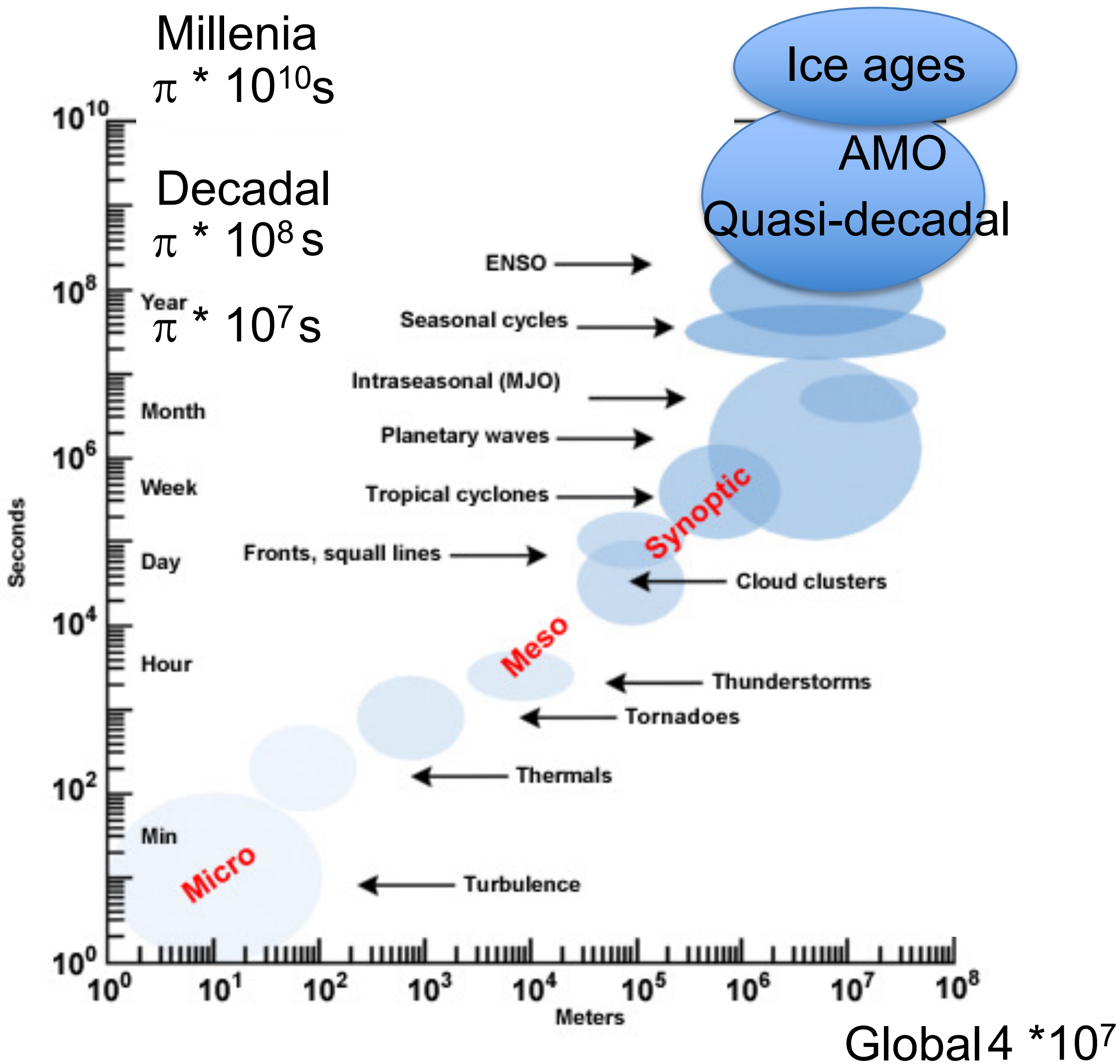

Spatial || temporal Scales

Optimal Fingerprints for the Detection of Time-dependent Climate Change

K. HASSELMANN

Max-Planck-Institut für Meteorologie, Hamburg, Germany

(Manuscript received 24 August 1992, in final form 17 March 1993)

$$f'_a = g'_a \sigma_a^{-2}. \tag{14}$$

The multiplication of the signal with the inverse of the covariance matrix is seen to weight the fingerprint components f'_a in the EOF frame relative to the signal components g'_a by the inverse σ_a^{-2} of the EOF variances, thereby slewing the fingerprint vector away from the EOF directions with high noise levels toward the low-noise directions.

Attribution (model world)

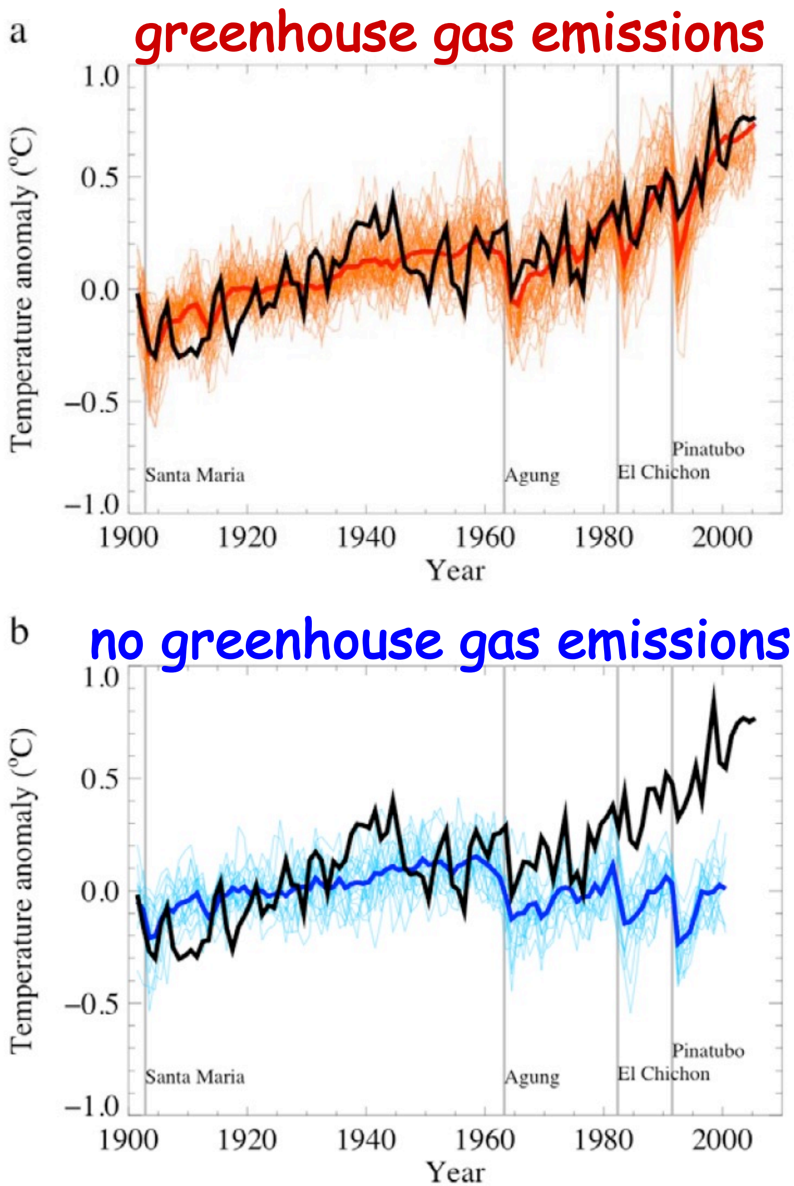

observed changes are consistent with modeled response to external forcing, inconsistent with alternative explanations

Nobel Price, 2021
Hasselmann

Attribution (model world)

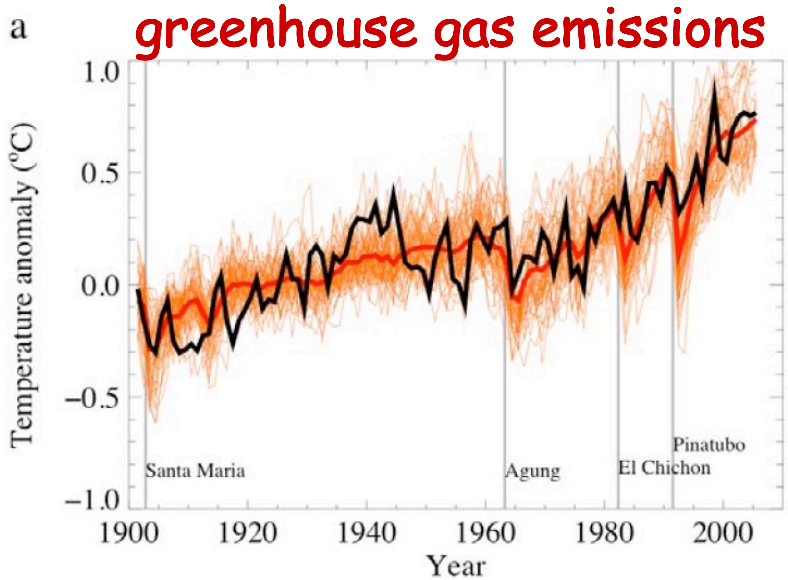

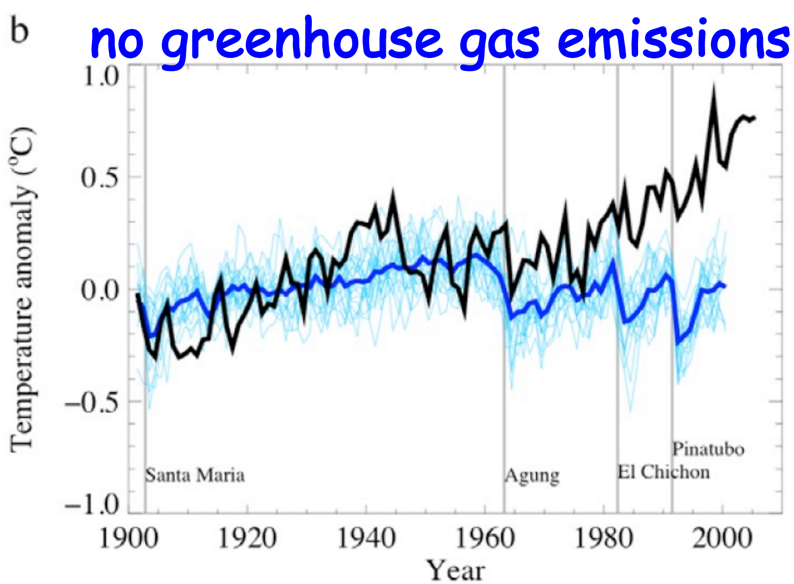

observed changes are consistent with modeled response to external forcing, inconsistent with alternative explanations

Critics:

- **Time series too short**
- **Estimates of natural variability based only on models**

Stochastic climate model (Hasselmann, 1976)

$$\frac{dT}{dt} = -\lambda T + \text{Noise} + \text{Forcing}$$

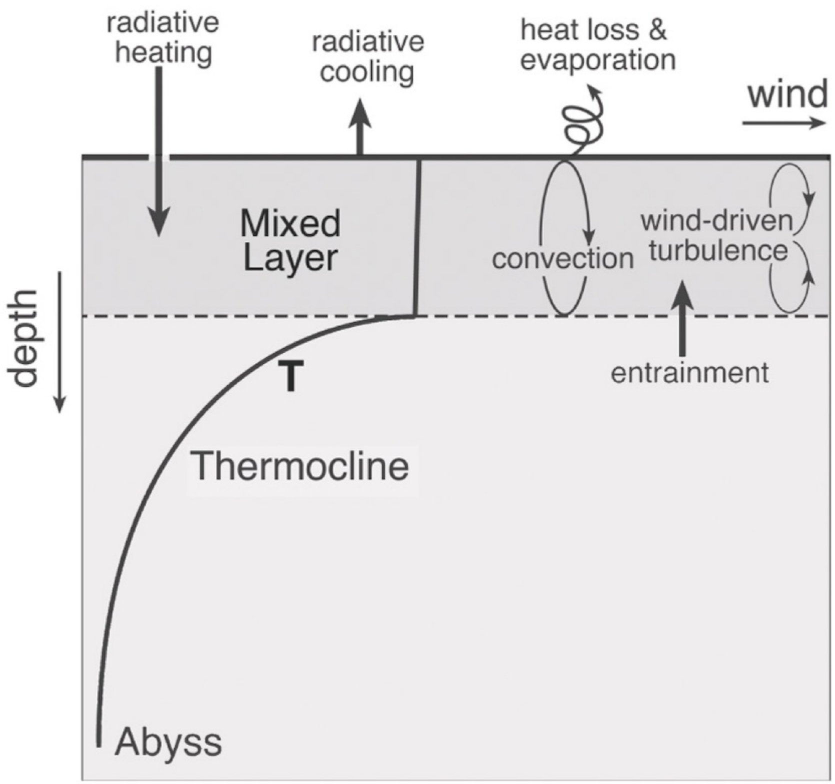

Figure 8.4: Schematic picture of mixed layer in the ocean.

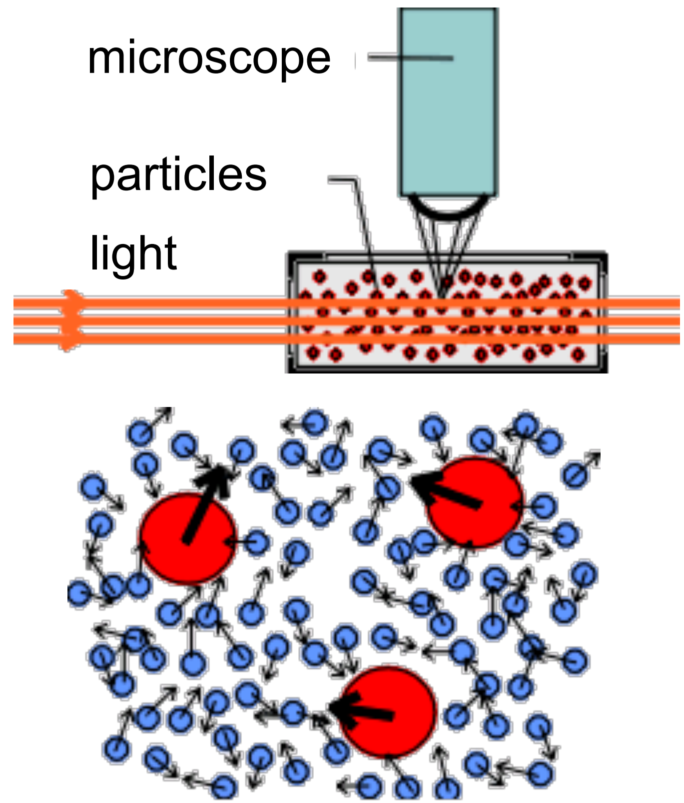

Disorderly, random motion
collision with molecules

5.2 STOCHASTIC PROCESSES

It is now time for time to appear in our discussion of random systems. When it does, this becomes the study of *stochastic processes*. We will look at two ways to bring in time: the evolution of probability distributions for variables correlated in time, and stochastic differential equations.

If $x(t)$ is a time-dependent random variable, its Fourier transform

$$X(\nu) = \lim_{T\to\infty} \int_{-T/2}^{T/2} e^{i2\pi\nu t} x(t)\, dt \tag{5.27}$$

is also a random variable but its *power spectral density* $S(\nu)$ is not:

$$\begin{aligned} S(\nu) &= \langle |X(\nu)|^2 \rangle = \langle X(\nu) X^*(\nu) \rangle \\ &= \lim_{T\to\infty} \frac{1}{T} \int_{-T/2}^{T/2} e^{i2\pi\nu t} x(t)\, dt \int_{-T/2}^{T/2} e^{-i2\pi\nu t'} x(t')\, dt' \end{aligned} \tag{5.28}$$

(where X^* is the complex conjugate of X, replacing i with $-i$). The inverse Fourier transform of the power spectral density has an interesting form,

$$\begin{aligned} &\int_{-\infty}^{\infty} S(\nu) e^{-i2\pi\nu\tau}\, d\nu \\ &= \int_{-\infty}^{\infty} \langle X(\nu) X^*(\nu) \rangle e^{-i2\pi\nu\tau}\, d\nu \\ &= \lim_{T\to\infty} \frac{1}{T} \int_{-\infty}^{\infty} \int_{-T/2}^{T/2} e^{i2\pi\nu t} x(t)\, dt \int_{-T/2}^{T/2} e^{-i2\pi\nu t'} x(t')\, dt'\, e^{-i2\pi\nu\tau}\, d\nu \end{aligned}$$

$$
\begin{aligned}
&= \lim_{T\to\infty} \frac{1}{T} \int_{-\infty}^{\infty} \int_{-T/2}^{T/2} \int_{-T/2}^{T/2} e^{i2\pi\nu(t-t'-\tau)}\, d\nu\, x(t)x(t')\, dt\, dt' \\
&= \lim_{T\to\infty} \frac{1}{T} \int_{-T/2}^{T/2} \int_{-T/2}^{T/2} \delta(t-t'-\tau) x(t)x(t')\, dt\, dt' \\
&= \lim_{T\to\infty} \frac{1}{T} \int_{-T/2}^{T/2} x(t)x(t-\tau)\, dt \\
&= \langle x(t)x(t-\tau)\rangle \quad ,
\end{aligned} \tag{5.29}
$$

found by using the Fourier transform of a *delta function*

$$
\int_{-\infty}^{\infty} e^{-i2\pi\nu t} \delta(t)\, dt = 1 \quad \Rightarrow \quad \delta(t) = \int_{-\infty}^{\infty} e^{i2\pi\nu t}\, dt \quad , \tag{5.30}
$$

where the delta function is defined by

$$
\int_{-\infty}^{\infty} f(x)\delta(x-x_0)\, dx = f(x_0) \quad . \tag{5.31}
$$

This is the *Wiener–Khinchin* theorem. It relates the spectrum of a random process to its *autocovariance function*, or, if it is normalized by the variance, the *autocorrelation function* (which features prominently in time series analysis, Chapter 16).

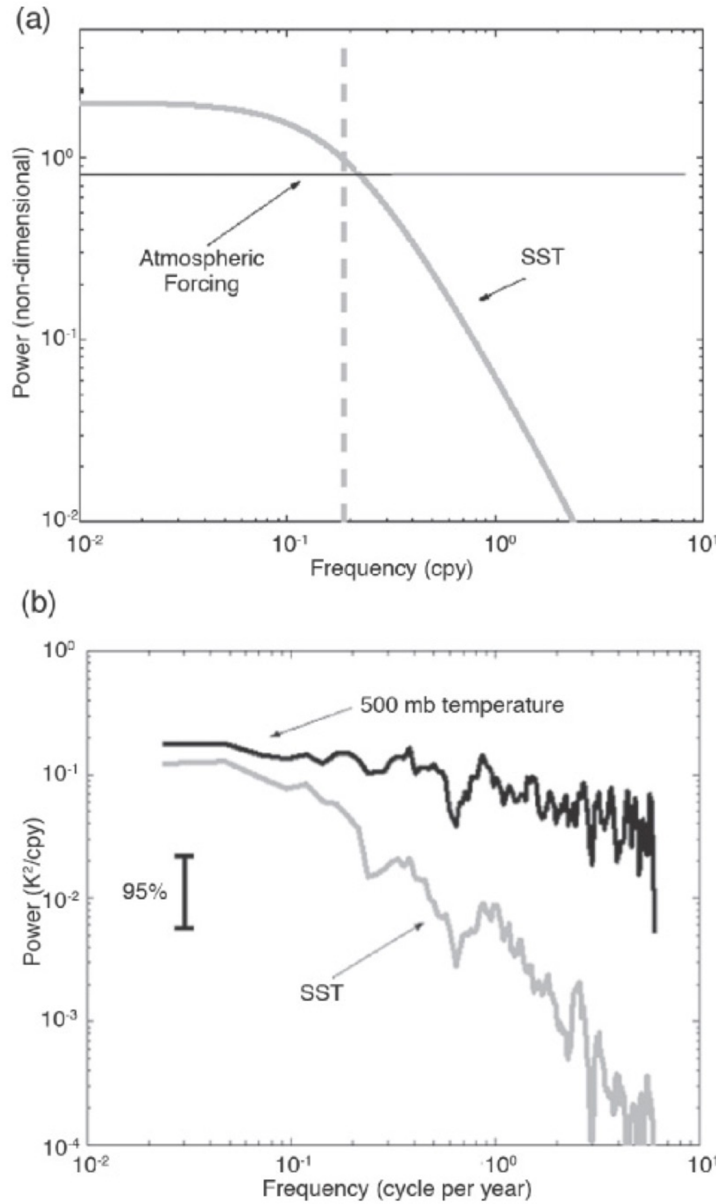

Figure 8.9: Powerspectrum of atmospheric temperature and sea surface temperature. Here $\mathbf{1/\lambda = 300}$ days from equation (8.43).

How realistic is the model?

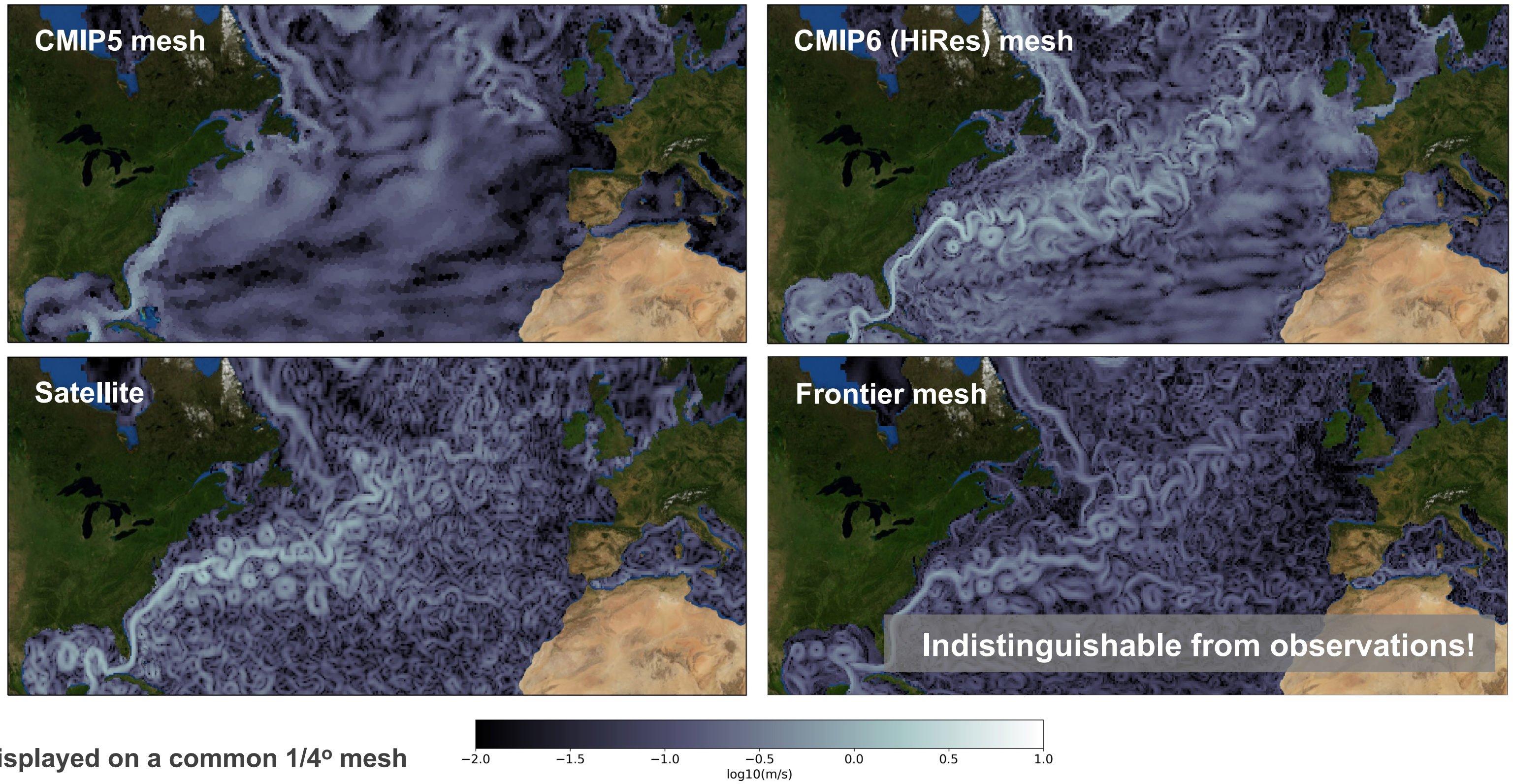

Displayed on a common 1/4º mesh

Ocean velocity

Scalability

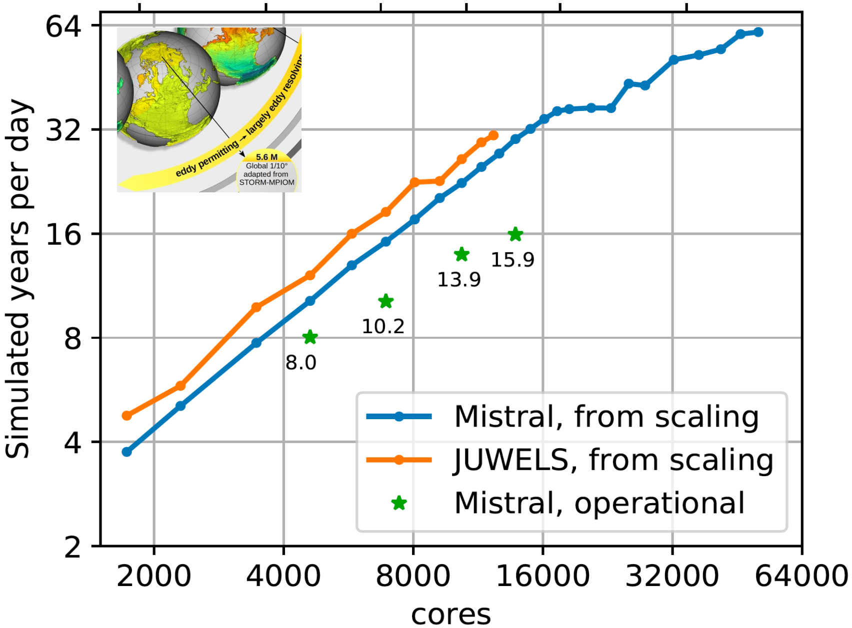

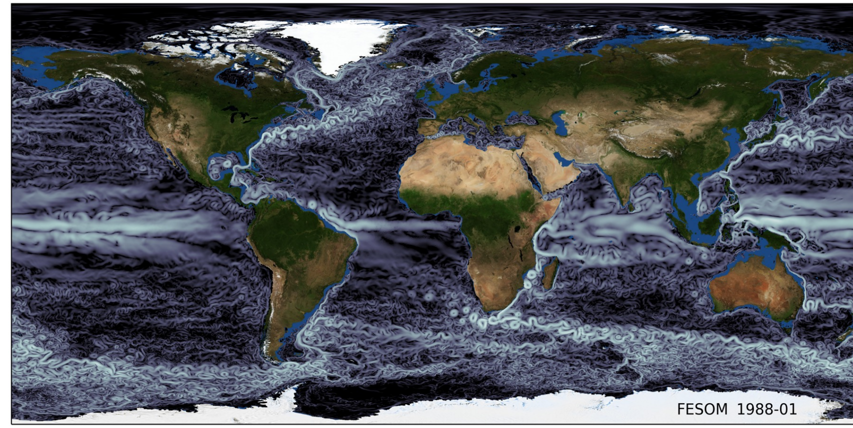

Koldunov et al (2019)

Limited by available HPC capabilities (today)

Limited by our ability to use future HPC systems (tomorrow)

Parameterizations

Some critical small-scale processes are *not* represented by the laws of physics, but by physically motivated rules of thumb (parametrizations)

➔ Large uncertainties in regional (global) climate change projections

➔ Limitations in predicting extreme events

Exercises

https://paleodyn.uni-bremen.de/study/MES/MES_random.html